Estimating the Uncertainties Due to Truncation in Planar Near-Field Holograms

Allen C. Newell

Nearfield Systems Inc.
19730 Magellan Dr. Torrance CA 90502

ABSTRACT

A combination of analysis and simulation are used to estimate the amplitude and phase errors in the hologram calculated from planar near-field data. The antenna hologram is modeled as the sum of a continuous function that essentially represents a correctly aligned antenna and one or more step function discontinuities located at elements that are misaligned. The spectrum of the step function can be calculated exactly from the assumed amplitude, phase, pulse width and location of the element. This spectrum is then filtered in k-space to simulate the effect of truncating the measurement plane. It is well known that the primary result of truncation is the filtering of real and evanescent plane waves beyond an angle defined by the antenna and measurement plane geometry.

Using the results of the analysis, a script program was developed for the NSI2000 software that would calculate the spectrum from the input parameters, perform the filtering and calculate the hologram using the Fast Fourier Transform. The change in the amplitude of the reconstructed hologram pulse is then used to determine the error that results in the calculated element amplitude and/or phase. Sample curves are generated to illustrate the technique.

Keywords: Antenna measurements, Measurement errors, Planar near-field, Phased arrays .

1 Introduction

It has been shown by measurements and simulation[1,2,3] that the truncation of planar near-field data is the major source of uncertainty in calculating the hologram using the inverse Fourier Transform. The truncation eliminates reliable information about the AUT sidelobes beyond an angle determined by the measurement geometry and filters out all information about the evanescent modes. This limits the resolution of discontinuities in the hologram and causes errors in the calculated amplitude and phase distributions. Past studies have not resulted in a method to estimate the magnitude of these errors for an arbitrary antenna and measurement geometry.

Using a combination of analysis and simulation a technique has been developed that gives an estimate of the uncertainty in the hologram due to truncation. The measured data is represented as the sum of a smoothly varying distribution and localized discontinuities in amplitude and phase. Truncation has a minor effect on the hologram of the smoothly varying part and analysis and simulation are used to estimate the effect of truncation on the hologram of the discontinuities.

2 Analysis

The measurement and calculations involved in determining the hologram of an antenna from planar near-field measurements are as follows:

Amplitude and phase data are obtained on a measurement plane that is generally at least a few wavelengths from the aperture, z = d, and denoted as $b(\vec{P})$, where $\vec{P}$ denotes the x,y position of the probe on the measurement plane. Data is generally obtained for two independent polarizations and the probe correction uses both the main and cross component properties of the probe. Since the cross component pattern of the probe has a very small effect on the main component results, we will use an approximate form of the probe correction in the following analysis to focus on the main features. The plane wave spectrum of the main component data is given by the Fourier transform relation,

$$D(\vec{K}) = \frac{e^{-i\gamma d}}{4\pi^2} \iint b(\vec{P}) e^{-i\vec{K}\bullet\vec{P}} d\vec{P} \qquad (1)$$

and the approximate probe correction is applied to give the plane wave transmitting spectrum of the AUT,

$$t(\vec{K}) = \frac{D(\vec{K})}{s(\vec{K})} \qquad (2)$$

In some cases, the AUT spectrum is divided by the element pattern if the antenna is a phased array, but this has a small effect on the final results and has virtually no effect on the influence of truncation errors, so this detail will also be neglected for simplicity. The hologram at z = z_0 is then given by,

$$h(\vec{P}, z = z_0) = \iint t(\vec{K}) e^{i\gamma z_0} e^{i\vec{K}\cdot\vec{P}} d\vec{K} \; . \qquad (3)$$

The primary error in the hologram calculation is due to filtering of the spectrum caused by the combination of truncation of the measured data and decay of the evanescent modes between the AUT aperture and the measurement plane. As a result of this filtering, the spectrum that is calculated by Equation (1) does not contain accurate values of $D(k_x, k_y)$ for the higher values of k_x and k_y. These values represent the wide-angle regions of real space and the evanescent region of imaginary space which should produce the detail and fine structure of the hologram.

To estimate the error caused by this filtering we will represent the measured data as the sum of two terms. The first term will represent the near-field of the AUT without any large discontinuities that arise from radiating elements that are either not operating or are incorrectly set. This term will represent a correctly operating and aligned antenna and will be a smoothly varying function of the probe position $\vec{P}$. The second term will represent the data on the measurement plane that is due to all the discontinuities in the aperture of the AUT and will be due to abrupt changes in amplitude and/or phase in the aperture plane. These abrupt changes will be smoothed out in the measurement plane by the filtering of the probe and the attenuation of the evanescent modes, but in principle, they could be accurately reconstructed from measurements over an infinite plane and perfect probe correction. The smooth and discontinuous terms will be denoted respectively as $b_s(\vec{P})$ and $b_d(\vec{P})$ and the resulting measured data, plane wave spectrum of the measured data and hologram are also composed of corresponding terms.

$$b(\vec{P}) = b_s(\vec{P}) + b_d(\vec{P}) \qquad (4)$$

$$t(\vec{K}) = t_s(\vec{K}) + t_d(\vec{K}) \qquad (5)$$

$$h(\vec{P}) = h_s(\vec{P}) + h_d(\vec{P}) \; . \qquad (6)$$

The far-out sidelobes and evanescent modes of the first term in Equation (5) will be very small compared to the main beam and therefore the filtering of the spectrum for this term will have very little effect on the hologram compared to the effect of filtering on the second term, (see Figure 3). We may therefore focus on just the second term to estimate truncation errors.

The detailed character of $b_d(\vec{P})$ will depend on the AUT aperture distribution, the number and location of discontinuities, the properties of the probe, and the distance from the aperture to the measurement plane. But the detailed character of the measured data is not the important quantity of interest. The important quantity is the hologram of the second term and how it compares to the hologram of the input discontinuity in the aperture plane.

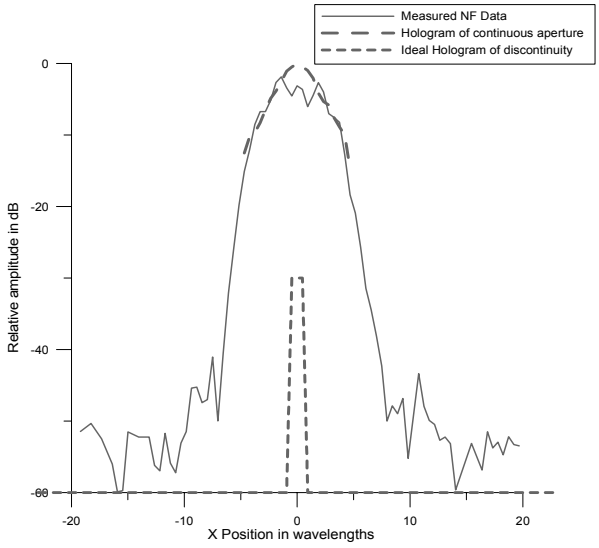

Figure 1 Example of measured near-field data and the two parts of the hologram

Figure 1 illustrates an x-cut of the measured data on a plane 3 wavelengths from an antenna with an aperture of 10 wavelengths. The near-field data shows some ripples due to a faulty element near the center of the aperture, but the location and magnitude of the fault are not localized in

the measured data. The two terms in Equation (6) are shown by the two dashed curves. The smooth part shown by the large dashed curve over the aperture region represents the continuous aperture distribution with no faults. The step function shown by the small dashed curve represents $h_d(\vec{P})$ and is the discontinuity due to a faulty element. The step function in Figure 1 is the hologram that would be calculated if there were no filtering of the calculated spectrum or other errors, and will be the standard that will be compared to the actual calculated results.

3 Simulation Results

The steps in the simulation will first be illustrated by the example of an antenna with only an amplitude error in one element.

$$\begin{aligned} h(\vec{P}) &= h_s(\vec{P}) + h_d(\vec{P}) \\ &= a_s(\vec{P})e^{i\phi_s(\vec{P})} + h_d(\vec{P}) \\ &= \left[a_s(\vec{P}) + a_e(\vec{P}) \right] e^{i\phi_s(\vec{P})} \end{aligned}$$

where (7)

$a_s(\vec{P}) =$ Amplitude of smooth term

$\phi_s(\vec{P}) =$ Phase of smooth term

$a_e(\vec{P}) =$ Amplitude error due to fault

and the second term is then defined in terms of the smooth function and the amplitude error.

$$h_d(\vec{P}) = a_e(\vec{P}_0)e^{i\phi_s(\vec{P})} \quad (8)$$

A near-field data file can be created with data that simulates $h_d(\vec{P})$ by initially setting all the amplitudes of an actual data set to zero except for a few data points centered on the location of the faulty element. The magnitude of the amplitude error can be adjusted by using different values of a_e, the location of the faulty element is chosen by $\vec{P}_0$, and the width of the discontinuity, corresponding to the dimensions of the radiating elements, can be set by the number of points that are not zero. Figure 2 shows an example of the input fault pulse for an element of 2 wavelengths at the center of the aperture. The magnitude has been set to the level of the original data, which in this case is –6 dB. The hologram is obtained by first calculating the spectrum for a square wave and reading these values into the far-field array. The spectrum is calculated analytically rather than

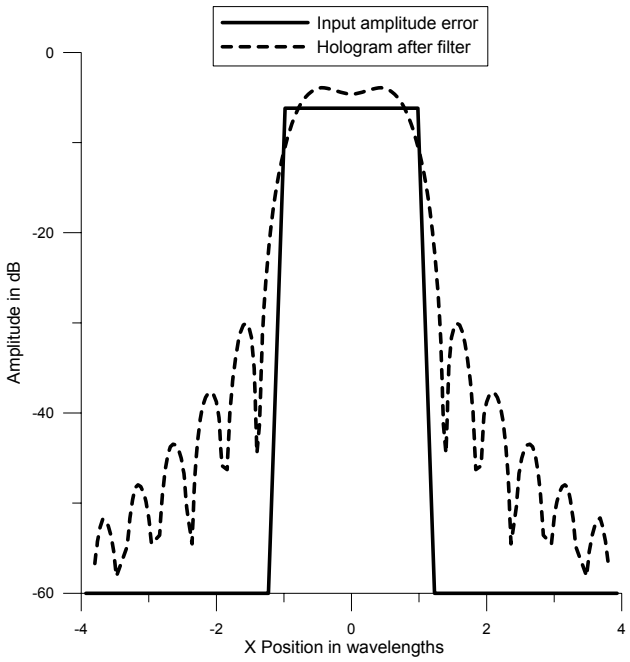

Figure 2 Example of amplitude error pulse and calculated hologram with filter at kx =ky=1.0.

using the FFT since the FFT does not give exact values for a square wave pulse. The calculated spectrum is an exact $\sin(x)/x$ function as shown in Figure 3. This exact spectrum is then filtered beyond a cutoff in both k_x and k_y to simulate the filtering due to truncation of the

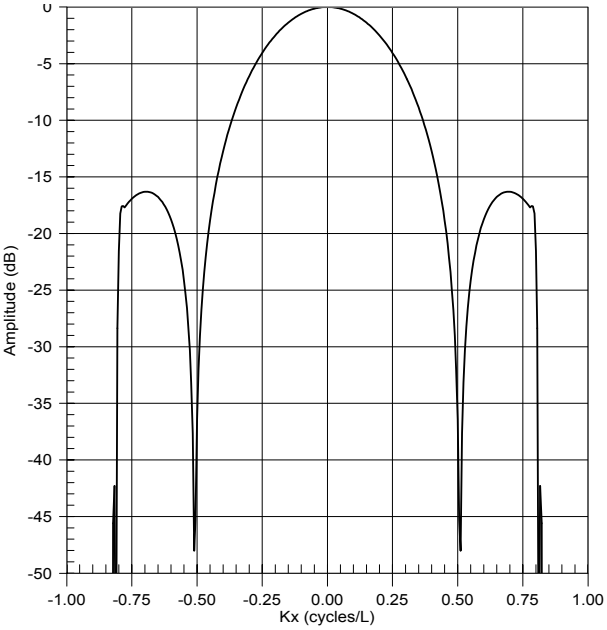

Figure 3 Spectrum of square wave filtered to kx = 0.8.

measurement plane, and the hologram is then calculated

from the filtered spectrum. The filter cutoff is related to the dimensions of the scan area L_x and L_y, the antenna aperture dimensions C_x and C_y, and the distance between the AUT and the scan plane d by the relations

$$\frac{|k_{x\max}|}{k} = \sin\left[arc\tan\left(\frac{L_x - C_x}{2d} \right)\right]$$
$$\frac{|k_{y\max}|}{k} = \sin\left[arc\tan\left(\frac{L_y - C_y}{2d} \right)\right] \quad (9)$$

A sample result for an element width of two wavelengths and a filter set at $k_{x\max}/k = k_{y\max}/k = 1.0$ is shown by the dashed line in Figure 2. This case shows the effect of filtering only the evanescent modes and represents the minimum error that would be approximated using a very large scan plane.

The amplitude error that results from this process is determined by solving Equation (8) for $a_e(\vec{P}_0)$ using the calculated value of the filtered hologram .

$$a_e(\vec{P}_0) = \frac{H_d(\vec{P}_0)}{e^{i\phi_s(\vec{P})}}$$
where (10)
$H_d(\vec{P}_0) =$ Value of filtered hologram at P_0

This calculated value is then compared with the input amplitude of the element that was used to produce the spectrum of the pulse. In the case of an amplitude error this is just comparing the amplitude of the square wave in Figure 2 to the amplitude of the filtered hologram. For the example in Figure 2 this gives an error in determining the element amplitude of 1.6 dB. This error is independent of the relative element amplitude and the same error would occur for all elements regardless of their individual excitation amplitudes. The error does depend on the size of the element and the filter limits, and Figure 4 shows the result of running the simulation for element dimensions from 0.5 to 2.0 wavelengths and for filter maximum of 0.5 to 1.0 which corresponds to cutoff angles of 30 degrees to 90 degrees.

The case of an element with only a phase error uses a similar process.

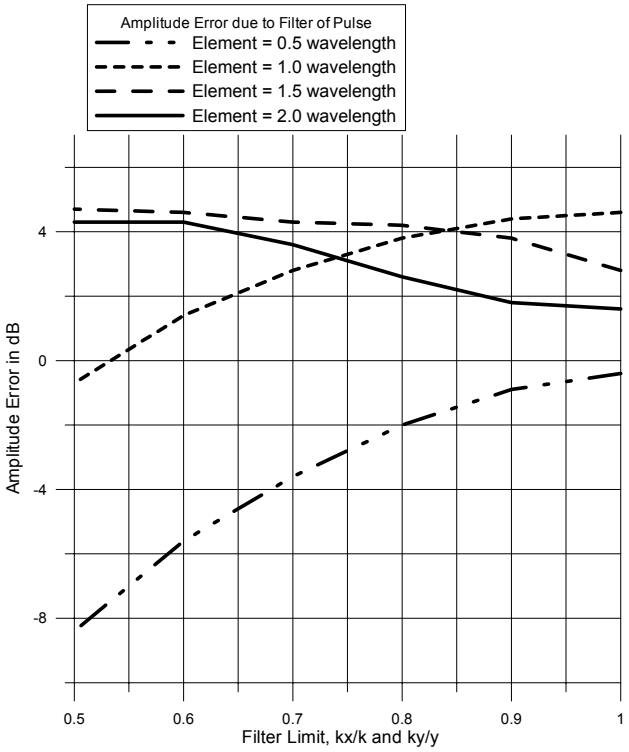

Figure 4 Results of simulation for elements with only amplitude errors.

The hologram is again modeled by the smooth term and the step discontinuities due to phase faults.

$$\begin{aligned} h(\vec{P}) &= h_s(\vec{P}) + h_d(\vec{P}) \\ &= a_s(\vec{P})e^{i\phi_s(\vec{P})} + h_d(\vec{P}) \\ &= \left[a_s(\vec{P}) \right] e^{i\left[\phi_s(\vec{P}) + \phi_e(\vec{P}_0)\right]} \end{aligned}$$
where (11)
$a_s(\vec{P}) =$ Amplitude of smooth term
$\phi_s(\vec{P}) =$ Phase of smooth term
$\phi_e(\vec{P}_0) =$ Element Phase error due to discontinuity

and the second term in Equation (6) is then given by

$$h_d(\vec{P}) = a_s(\vec{P}_0)e^{i\phi_s(\vec{P})}\left[e^{i\phi_e} - 1 \right] \quad (12)$$

and the hologram phase error is then given by

$$\phi_e = \arg\left[\frac{H_d(\vec{P}_0)}{a_s(\vec{P}_0)e^{i\phi_s(\vec{P})}} + 1\right]$$

where (13)

$H_d(\vec{P}_0) =$ Amplitude and Phase of filtered hologram at P_0

In this case, the input pulse representing the faulty element phase fault has an amplitude and phase equal to the smooth term but modified by the factor in the square brackets of Equation (12), $\left[e^{i\phi_e} - 1\right]$. If the element phase discontinuity is zero, there is no input pulse, but for other phases, both the amplitude and phase of the input pulse are changed. The filtering and inverse transform of the pulse spectrum will not change the phase of the hologram from its input value, but the amplitude is changed just like the example in Figure 2. When we then solve for the element phase using the changed amplitude and Equation (13) we obtain,

$$\begin{aligned}\phi_e &= \arg\left[\frac{H_d(\vec{P}_0)}{a_s(\vec{P}_0)e^{i\phi_s(\vec{P})}} + 1\right] \\ &= \arg\left[\frac{a'_s(\vec{P}_0)e^{i\phi_s(\vec{P})}\left[e^{i\phi_e} - 1\right]}{a_s(\vec{P}_0)e^{i\phi_s(\vec{P})}} + 1\right] \\ &= \arg\left[\frac{a'_s(\vec{P}_0)\left[e^{i\phi_e} - 1\right]}{a_s(\vec{P}_0)} + 1\right] \end{aligned} \quad (14)$$

where

$a'_s(\vec{P}_0) =$ amplitude of filtered hologram

If the input and output amplitudes are equal, there is no phase error, but if not, the phase error will depend on both the amplitude ratio and the element phase.

The phase error in the filtered hologram will depend on the element dimensions, the filter limits and the element phase. A graph like Figure (4) must therefore be generated for each element dimension. One sample graph for an element of 0.5 wavelengths is shown in Figure 5. The element phase as defined for this analysis is the difference between the smooth function phase and the actual element phase and is therefore the difference between the phase of a correctly aligned antenna and the actual element phase. The hologram phase error is largest for element phases of 90 and 270 degrees and least for element phases of 0 and 180 degrees.

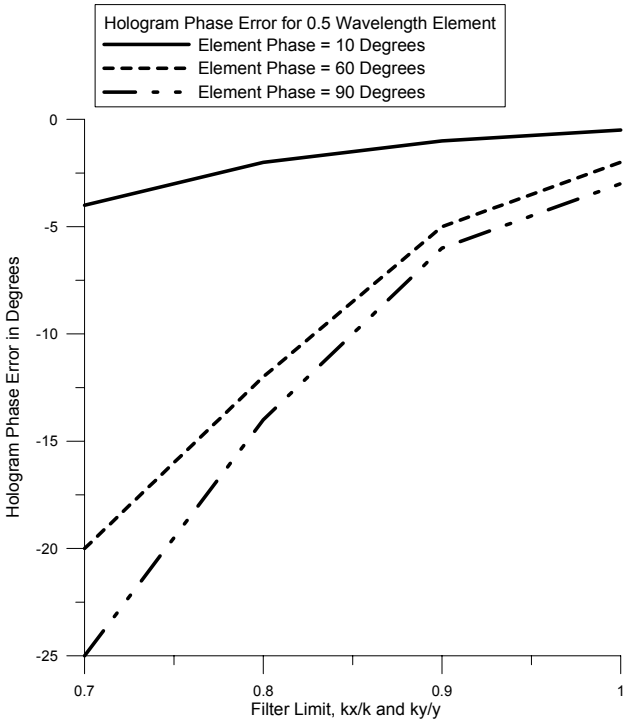

Figure 5 Hologram phase error for 0.5 wavelength element for typical filter limits.

The other error that has not been discussed here is the influence that the hologram of the filtered pulse has on other elements near the fault. As seen in Figure 2, the sidelobes of the filtered pulse extend beyond the boundaries of the faulty element and will have some effect on the reconstructed amplitude and phase of nearby elements. The extent of this influence will depend on the magnitude of the fault, the element dimensions and spacing and the filter limits. Examples of these effects will be studied in the future.

4 Conclusions

Using the developed analysis and simulation it is possible to predict the uncertainty in the hologram calculated from near-field measurements due to the truncation of the measurement plane. The scan geometry defines the cutoff angle of the measured spectrum and from the element size and the element fault magnitudes and phases uncertainty estimates can be derived.

5 References

[1] C. A. Rose, “Accuracy estimations of microwave holography from planar near-field measurements”, AMTA Proceedings 2000, p. 12, Philadelphia, PA, Oct 2000.

[2] D. Janes van Rensburg, Limitations of near-field back projection for phased array tuning applications”, ”, AMTA Proceedings 2001, Denver, CO, Oct 2001.

[3] M. H. A. Paquay, “Locating defective array modules using planar near-field measurements”, AMTA Proceedings 1998, Montreal, QC, Canada, Oct 1998.